

A comprehensive study of B , B_s & B_c meson semitauonic modes in potential quark model

Sonali Patnaik^{a,*}

^aIndian Institute of Technology, North Guwahati, Guwahati 781039, Assam, India

E-mail: spatnaik@iitg.ac.in

In this work, we derive the form factors and compute the branching fractions for the semitauonic decay modes, $B \rightarrow D^{(*)} \tau \nu_\tau$, $B_s \rightarrow D_s^{(*)} \tau \nu_\tau$, $B_c \rightarrow \eta_c (J/\psi) \tau \nu_\tau$, and $B_c \rightarrow D^{(*)} \tau \nu_\tau$ within the *Relativistic Independent Quark (RIQ) Model*, emphasizing a quark potential model based analysis of these transitions. We outline the essential elements of the model, incorporating corrections from residual interactions and center-of-mass motion, and perform a comprehensive study of the form factors across the full physical kinematic range of q^2 . The resulting predictions demonstrate consistency and good agreement with existing theoretical approaches and experimental measurements. Motivated by recent observations of polarization observables at LHCb and Belle, we further evaluate these quantities within our framework and find results compatible with Standard Model (SM) expectations. The predictions presented here serve as theoretical input in decay channels for which lattice QCD results remain limited, offering guidance for future experimental and Lattice efforts. Thus, semileptonic B decays continue to serve as precise and discerning probes of the fundamental mechanisms governing flavor transitions in the SM.

Proceedings of the Corfu Summer Institute 2025 "School and Workshops on Elementary Particle Physics and Gravity" (CORFU2025)
27 April - 28 September, 2025
Corfu, Greece

*Speaker

Weak decays of B , B_s , and B_c mesons containing a bottom (b) quark and spectator quarks (u, d, s, c) serve as excellent probes of understanding physics within the SM and beyond (BSM). These decays test lepton flavor universality, as their SM predictions arise from clean tree-level processes. Recent deviations observed in $b \rightarrow c\ell\nu$ and $b \rightarrow s\ell\nu$ transitions have generated interest in flavor anomalies. Measurements of τ polarization $P_\tau(D^*)$ [1, 2] and fraction of longitudinal polarization $F_L^{D^*}$ are consistent with SM expectations [3, 4], as reaffirmed by LHCb [5]. Since $B_s \rightarrow D_s^{(*)}\ell\nu_\ell$ and $B \rightarrow D^{(*)}\ell\nu_\ell$ proceed via the same $b \rightarrow c\ell\nu_\ell$ transition, SU(3) flavor symmetry [6] implies similar semileptonic behavior. Any new physics effects in $B \rightarrow D^{(*)}\ell\nu$ should thus also appear in $B_s \rightarrow D_s^{(*)}\ell\nu$ channels due to SU(3) flavor symmetry effects. Observables such as $P_\tau(D_s^{(*)})$ and $F_L(D_s^*)$ therefore provide complementary sensitivity to BSM effects, while the sizable decay width of $B_c \rightarrow \eta_c (J/\psi) \bar{\ell} \nu_\ell$ makes it another promising probe [7, 8]. On the theoretical side, weak decays offer a crucial means to determine transition form factors using non-perturbative methods such as the Bethe–Salpeter equation (BSE), QCD sum rules (QCDSRs), and Lattice QCD (LQCD). Combining HQET and QCDSRs allows estimates for $B \rightarrow D\tau\nu_\tau$, though with limited precision [9]. Besides, QCD-inspired quark models remain valuable tools when they successfully reproduce experimental data across hadron sectors. Motivated by ongoing B -physics efforts, we therefore investigate exclusive semileptonic decays of b -flavored mesons using the Relativistic Independent Quark (RIQ) model. We compute the semileptonic decays: $B \rightarrow D^{(*)}$, $B_s \rightarrow D_s^{(*)}$, $B_c \rightarrow \eta_c (J/\psi)$ and $B_c \rightarrow D^{(*)}$ focusing on τ modes governed by six Lorentz invariant form factors. These are extracted in the RIQ model as overlap integrals of meson wave functions [10, 11]. We evaluate them over the full physical kinematic range of q^2 and present branching fractions, form factors and angular observables for τ modes. In the absence of sufficient LQCD data, our analysis offers valuable SM predictions that enhance the understanding of semileptonic B decays, particularly in channels involving third-generation leptons.

1. RIQ model framework

Studying exclusive semileptonic decays involving non-perturbative hadronic matrix elements can be defined using confining interaction potential formulation. In this context, we provide a concise theoretical predictions adopting the RIQ model (RIQM) framework. The RIQM is grounded in a confining harmonic potential in the equally mixed scalar-vector form [10, 12, 13],

$$U(r) = \frac{1}{2} \left(1 + \gamma^0 \right) V(r), \quad V(r) = (ar^2 + V_0). \quad (1)$$

Here, r represents a state dependent length parameter, γ^0 denotes the time-like Hermitian matrix, a and V_0 are potential parameters. These parameters are fixed during the hadron spectroscopy [14]. This confining interaction is believed to provide phenomenologically the zeroth order quark dynamics inside the hadron-core through the quark Lagrangian density, This confining interaction is believed to provide phenomenologically the zeroth order quark dynamics inside the hadron-core through the quark Lagrangian density,

$$\mathcal{L}_q^0(x) = \bar{\psi}_q(x) \left[\frac{i}{2} \gamma^\mu \partial_\mu - m_q - U(r) \right] \psi_q(x), \quad (2)$$

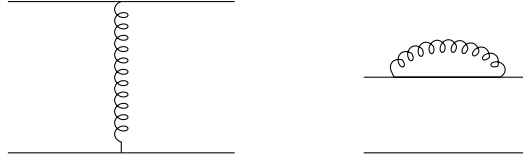


Figure 1: One gluon exchange contribution to the energy of $q\bar{q}$ configuration

leading to the Dirac equation for individual quark & antiquark systems. Since first principle QCD calculations remain challenging due to its non-perturbative nature therefore RIQM derives observable hadron properties from constituent quark dynamics. The model characterizes quark confinement through the chosen potential in Eq. (1), representing multi-gluon interactions with a specified Lorentz structure. Residual effects such as one-gluon exchange (OGE) at short distances and quark–pion coupling in the light sector are treated perturbatively [15, 16]. As the present work focuses on heavy hadrons pionic contribution becomes negligible and only the OGE term is considered. Therefore in the next section we briefly describe the OGE within the RIQM.

1.1 One gluon-exchange correction

Within the meson core quarks experience the effective potential $U(r)$ along with a residual weak OGE interaction as depicted in Fig. 1 from the interaction Lagrangian density,

$$\mathcal{L}_I^g = \sum_a J_i^{\mu a}(x) A_\mu^a(x), \quad (3)$$

where $A_\mu^a(x)$ are vector-gluon fields and $J_i^{\mu a}(x)$ is the i th-quark colour-current. Since at small distances the quarks should be almost free, it is reasonable to calculate the shift in energy of the meson-core arising out of the quark interaction energy due to its coupling to the coloured gluons, using a first order perturbation theory. Such an approach leads to the colour-electric and colour-magnetic energy shifts [15, 16].

$$(\Delta E_M)_g = (\Delta E_M)_g^{\mathcal{E}} + (\Delta E_M)_g^{\mathcal{M}}, \quad (4)$$

$$(\Delta E_M)_g^{\mathcal{E}} = \alpha_s \sum_{i,j} \left\langle \sum_a \lambda_i^a \lambda_j^a \right\rangle \frac{1}{\sqrt{\pi} R_{ij}} \left(1 - \frac{\alpha_i + \alpha_j}{R_{ij}^2} + \frac{3\alpha_i \alpha_j}{R_{ij}^4} \right), \quad (5)$$

$$(\Delta E_M)_g^{\mathcal{M}} = \alpha_s \sum_{i < j} \left\langle \sum_a \lambda_i^a \lambda_j^a \boldsymbol{\sigma}_i \cdot \boldsymbol{\sigma}_j \right\rangle \frac{256}{9\sqrt{\pi}} \frac{1}{(3E'_i + m'_i)(3E'_j + m'_j)} \frac{1}{R_{ij}^3}. \quad (6)$$

Here λ_i^a denote the Gell-Mann SU(3) matrices and α_s represents the effective scale-dependent strong coupling constant. Considering the specific flavor and spin configurations of ground-state mesons, the corresponding OGE energy correction $(\Delta E_M)_g$ is obtained. This would give the total energy of $(q_i \bar{q}_j)$ system in its ground state as,

$$E_M = E_M^0 + [(\Delta E_M)_g^{\mathcal{E}} + (\Delta E_M)_g^{\mathcal{M}}], \quad (7)$$

where E_M^0 is the zeroth order energy for a ground-state meson M arising out of the binding energies of constituent quark and antiquark confined independently by average potential $U(r)$. We further incorporate the correction from the spurious center-of-mass motion of $q\bar{q}$ system, detailed below.

1.2 Centre of mass momentum and meson mass

In this shell-type relativistic independent quark model, the motion of individual quarks within the hadron core does not inherently result in a state with a well-defined total momentum as required for a physically consistent hadron state. Therefore, the energy contribution from the spurious center-of-mass motion must be accounted as an additional correction to the hadron energy, obtained from the individual quark binding energy over and above the perturbative corrections discussed in 1.1. This correction has been thoroughly detailed in the earlier work [15].

In such an approach, the static meson-core state with core-centre at X is decomposed into components $\Phi(P)$ of plane-wave momentum eigen states as,

$$|M(X)\rangle_c = \int \frac{d^3P}{W_M(P)} \exp(iP \cdot X) \Phi_M(P) |M(P)\rangle. \quad (8)$$

Taking its inverse relation along with the normalisation, one can obtain the momentum profile function $\Phi_M(P)$ as,

$$\Phi_M^2(P) = \frac{W_M(P)}{(2\pi)^3} \tilde{I}_M(P), \quad (9)$$

where $\tilde{I}_M(P)$ is the fourier-transform of the Hill-wheeler overlap function [17] given by,

$$\tilde{I}_M(P) = \left(\frac{r_{0q}^2}{2\pi} \right)^{3/2} \exp(-P^2 r_{0q}^2 / 2) (1 - 6C_q + 15C_q^2) \left[1 + \frac{P^2 r_{0q}^2 (2C_q - 10C_q^2 + C_q^2 P^2 r_{0q}^2)}{(1 - 6C_q + 15C_q^2)} \right], \quad (10)$$

when, $C_q = (E'_q - m'_q)/6(3E'_q + m'_q)$. We now estimate the center-of-mass momentum P as,

$$\langle P^2 \rangle = \int d^3P \tilde{I}_M(P) P^2 = \sum_q \langle p^2 \rangle. \quad (11)$$

$\langle p^2 \rangle$ is the average value of the square of the individual quark-momentum taken over $1S_{1/2}$ single-quark state and is given by,

$$\langle p^2 \rangle_q = \frac{(11E'_q + m'_q)(E_q^{2'} - m_q^{2'})}{6(3E'_q + m'_q)}. \quad (12)$$

Finally taking into account the centre-of-mass motion of $(q_i \bar{q}_j)$ system with the center-of-mass momentum P as in Eq. 11 & 12, one can obtain the physical mass of $(q_i \bar{q}_j)$ meson in its ground state as,

$$m_M = [E_M^2 - \langle P^2 \rangle_M]^{1/2}. \quad (13)$$

By including residual interaction effects and center-of-mass corrections, the model reliably reproduces the meson spectrum across various S-wave states through fitted quark masses and potential parameters, in good agreement with experimental data [18, 19]. The extended RIQM framework thus provides a robust phenomenological tool for studying hadronic properties. Since the focus of this work is on semileptonic decay observables, we abstain from presenting a detailed mass spectrum analysis and instead concentrate on predicting branching fractions and form factors for the relevant decay channels.

2. Theoretical setup for the weak decays in RIQM

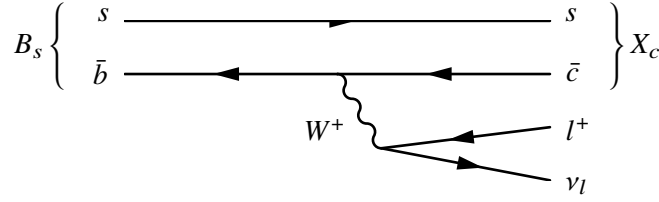


Figure 2: Leading order Feynman diagram for $B_q \rightarrow X_q \tau \nu_\tau$

The invariant transition matrix element for $B_q \rightarrow X_q \tau \nu_\tau$, where q represent the spectator quarks $q = u, d, s, c$, governing by the quark level transition $b \rightarrow c(u) \tau \nu_\tau$ as depicted in Fig. 2, is expressed as,

$$\mathcal{M}(p, k, k_\tau, k_{\nu_\tau}) = \frac{\mathcal{G}_F}{\sqrt{2}} V_{c(u)b} \mathcal{H}_\mu(p, k) \mathcal{L}^\mu(k_\tau, k_{\nu_\tau}), \quad (14)$$

Here \mathcal{G}_F is the effective Fermi coupling constant, $V_{c(u)b}$ the relevant CKM matrix element, and \mathcal{L}^μ and \mathcal{H}_μ denote the leptonic and hadronic currents, respectively. The four-momenta $p, k, k_\tau, k_{\nu_\tau}$ correspond to the parent meson $B_q = (B, B_s, B_c)$, daughter meson $X = \{D (D^*), D_s (D_s^*), \eta_c (J/\psi)\}$, τ lepton, and neutrino. In decay processes, mesons are described as momentum-space wave packets representing quark–antiquark momentum and spin distributions. Within the RIQM, the meson bound state $|B(\vec{p}, S_B)\rangle$ is expressed as [10],

$$|B(\vec{p}, S_B)\rangle = \hat{\Lambda}(\vec{p}, S_B) |(\vec{p}_b, \lambda_b); (\vec{p}_d, \lambda_d)\rangle, \quad (15)$$

$$\hat{\Lambda}(\vec{p}, S_B) = \frac{\sqrt{3}}{\sqrt{N(\vec{p})}} \sum_{\lambda_b, \lambda_d} \zeta_{b,d}^B(\lambda_b, \lambda_d) \int d^3 p_b d^3 p_d \delta^{(3)}(\vec{p}_b + \vec{p}_d - \vec{p}) \mathcal{G}_{B_s}(\vec{p}_b, \vec{p}_d)$$

Here, $\sqrt{3}$ is the color factor, and $\zeta_{b,d}^B(\lambda_b, \lambda_d)$ the SU(6) spin–flavor coefficient of the B meson. $|(\vec{p}_b, \lambda_b); (\vec{p}_d, \lambda_d)\rangle$ denotes the Fock-space state of a color-singlet quark–antiquark pair with their respective momentum and spin, $\hat{\Lambda}(\vec{p}, S_B)$ encoding the meson’s bound-state structure. The same structure can be extended to other meson states: $B_u, B_s, B_c, D, D_s, \eta_c$, and J/ψ . Hadronic matrix elements for transitions between hadrons of definite spin and parity are expressed as tensor structures multiplied by form factors which encode non-perturbative dynamics [9]. For $0^- \rightarrow 0^-$ and $0^- \rightarrow 1^-$ transitions, the processes involve two and four independent form factors, respectively, defined for the vector and axial-vector currents.

$$\begin{aligned} \langle D (D_s) | \bar{c} \gamma_\mu b | B (B_s) \rangle &= (p+k)_\mu f_+(q^2) + q_\mu f_-(q^2), \\ \langle D^* (D_s^*) | \bar{c} \gamma_\mu b | B (B_s) \rangle &= \frac{1}{M+m} \epsilon^{\sigma+} \left\{ i \epsilon_{\mu\sigma\alpha\beta} (p+k)_\alpha q_\beta V(q^2) \right\}, \\ \langle D^* (D_s^*) | \bar{c} \gamma_\mu \gamma_5 b | B (B_s) \rangle &= \frac{1}{M+m} \epsilon^{\sigma+} \left\{ g_{\mu\sigma} (p+k)_\mu q_\mu A_0(q^2) + \right. \\ &\quad (p+k)_\mu (p+k)_\sigma A_+(q^2) + \\ &\quad \left. q_\mu (p+k)_\sigma A_-(q^2) \right\}. \end{aligned} \quad (16)$$

The hadronic amplitude \mathcal{H}_μ in (14) is derived by evaluating the overlap integral of the meson wave-

functions as in (15) and in the parent meson rest frame, obtained as,

$$\mathcal{H}_\mu = \sqrt{\frac{ME_k}{N_B(0)N_X(\vec{k})}} \int \frac{d^3p_b}{\sqrt{E_{p_b}E_{k+p_b}}} \mathcal{G}_B(\vec{p}_b, -\vec{p}_d) \mathcal{G}_X(\vec{k} + \vec{p}_b, -\vec{p}_d) \langle S_X | J_\mu^h(0) | S_B \rangle. \quad (17)$$

Here, E_{p_b} and E_{k+p_b} are the energies of the non-spectator quark in the parent and daughter mesons, respectively, and $\langle S_X | J_\mu^h(0) | S_B \rangle$ denotes the spin matrix elements of the hadronic vector-axial vector current. For $0^- \rightarrow 0^-$ and $0^- \rightarrow 1^-$ transitions, these matrix elements are independently obtained from the RIQM and after comparing with the covariant expansion of form factors Eq. (16), yields the model expressions for the form factors $f_\pm(q^2)$, $V(q^2)$, $A_0(q^2)$, $A_+(q^2)$, and $A_-(q^2)$.

$$\begin{aligned} f_\pm(q^2) &= \frac{1}{2M} \sqrt{\frac{ME_k}{N_B(0)N_X(\vec{k})}} \int d\vec{p}_b \mathcal{G}_B(\vec{p}_b, -\vec{p}_d) \mathcal{G}_X(\vec{k} + \vec{p}_b, -\vec{p}_d) \\ &\quad \times \frac{(E_{p_b} + m_b)(E_{p_c} + m_c) + |\vec{p}_b|^2 \pm (E_{p_b} + m_b)(M \mp E_k)}{E_{p_b}E_{p_c}(E_{p_b} + m_b)(E_{p_c} + m_c)}, \\ V(q^2) &= \frac{M + m}{2M} \sqrt{\frac{ME_k}{N_B(0)N_X(\vec{k})}} \int d\vec{p}_b \mathcal{G}_B(\vec{p}_b, -\vec{p}_d) \mathcal{G}_X(\vec{k} + \vec{p}_b, -\vec{p}_d) \\ &\quad \times \sqrt{\frac{E_{p_b} + m_b}{E_{p_b}E_{p_c}(E_{p_c} + m_c)}}, \\ A_0(q^2) &= \frac{1}{M - m} \sqrt{\frac{Mm}{N_B(0)N_X(\vec{k})}} \int d\vec{p}_b \mathcal{G}_B(\vec{p}_b, -\vec{p}_d) \mathcal{G}_X(\vec{k} + \vec{p}_b, -\vec{p}_d) \\ &\quad \times \frac{(E_{p_b} + m_b)(E_{p_c}^0 + m_c) - \frac{|\vec{p}_b|^2}{3}}{\sqrt{E_{p_b}E_{p_c}(E_{p_b} + m_b)(E_{p_c} + m_c)}}, \\ A_\pm(q^2) &= \frac{-E_k(M + m)}{2M(M + 2E_k)} \left[T \mp \frac{3(M \mp E_k)}{E_k^2 - m^2} \{I - A_0(M - m)\} \right], \\ T &= J - \frac{M - m}{E_k} A_0, \\ J &= \sqrt{\frac{ME_k}{N_B(0)N_X(\vec{k})}} \int d\vec{p}_b \mathcal{G}_B(\vec{p}_b, -\vec{p}_d) \mathcal{G}_X(\vec{k} + \vec{p}_b, -\vec{p}_d) \sqrt{\frac{E_{p_b} + m_b}{E_{p_b}E_{p_c}(E_{p_c} + m_c)}}, \\ I &= \sqrt{\frac{ME_k}{N_B(0)N_X(\vec{k})}} \int d\vec{p}_b \mathcal{G}_B(\vec{p}_b, -\vec{p}_d) \mathcal{G}_X(\vec{k} + \vec{p}_b, -\vec{p}_d) \\ &\quad \times \frac{(E_{p_b} + m_b)(E_{p_c}^0 + m_c) - \frac{|\vec{p}_b|^2}{3}}{\sqrt{E_{p_b}E_{p_c}(E_{p_b} + m_b)(E_{p_c}^0 + m_c)}}, \\ \text{where } E_{p_c}^0 &= \sqrt{|\vec{p}_c|^2 + m_c^2}. \end{aligned} \quad (18)$$

With the relevant form factors thus obtained in terms of model quantities, the helicity amplitudes and hence the semitauonic decay rates for $B \rightarrow D^{(*)}$, $B_s \rightarrow D_s^{(*)}$, $B_c \rightarrow \eta_c(J/\psi)$ and $B_c \rightarrow D^{(*)}$ are evaluated in the following section and our predictions are listed in section 3.

2.1 Helicity amplitudes & decay distribution

Using the weak form factors (18), the angular decay distribution in q^2 is expressed as,

$$\frac{d\Gamma}{dq^2 d\cos\theta} = \frac{\mathcal{G}_F^2}{(2\pi)^3} |V_{c(u)b}|^2 \frac{(q^2 - m_\tau^2)^2}{8M^2 q^2} |\vec{k}| \mathcal{L}^{\mu\sigma} \mathcal{H}_{\mu\sigma}, \quad 0 \leq q^2 \leq (M - m)^2, \quad (19)$$

where $q = p - k = k_\tau + k_{\nu_\tau}$. M , m and m_τ denote the parent & daughter meson and τ -lepton masses, respectively. For convenience the lepton-hadron structure tensors are written in helicity space after utilizing the completeness property,

$$\mathcal{L}^{\mu\sigma} \mathcal{H}_{\mu\sigma} = \mathcal{L}_{\mu'\sigma'} g^{\mu'\mu} g^{\sigma'\sigma} \mathcal{H}_{\mu\sigma} = L(m, n) g_{mm'} g_{nn'} H(m', n'), \quad (20)$$

$$L(m, n) = \epsilon^\mu(m) \epsilon^{\sigma\dagger}(n) \mathcal{L}_{\mu\sigma}, \quad H(m, n) = \epsilon^{\mu\dagger}(m) \epsilon^\sigma(n) \mathcal{H}_{\mu\sigma}. \quad (21)$$

The helicity form factors are obtained by projecting the Lorentz invariant form factors onto the helicity states of the final particles. The Lorentz index contraction in Eq. (19) is then performed using these helicity amplitudes linking the covariant and helicity formulations [10]. The azimuthal angle χ of the lepton pair is omitted and integrating over χ simplifies the decay distribution to depend only on q^2 and the lepton polar angle θ . The differential partial helicity rates $d\Gamma_i/dq^2$ thus reduce to the form:

$$\frac{d\Gamma_i}{dq^2} = \frac{\mathcal{G}_F^2 |V_{c(u)b}|^2}{(2\pi)^3} \frac{(q^2 - m_\tau^2)^2}{12M^2 q^2} |\vec{k}| H_i. \quad (22)$$

H_i denotes the conventional set of helicity structure functions each defined as a specific linear combination of the helicity components of hadronic tensor involving the respective form factors.

$$H_U = H_+^2 + H_-^2, \quad H_L = H_0^2, \quad H_P = H_+^2 - H_-^2, \quad H_S = 3H_t^2, \quad H_{SL} = H_t H_0, \quad (23)$$

With this definition of the helicity components, required relations between the helicity form factors and the Lorentz invariant form factors can be expressed as follows,

$$\begin{aligned} H_t &= \epsilon^{\mu\dagger}(t) \epsilon_2^{\alpha\dagger}(0) \mathcal{H}_{\mu\alpha} \\ &= \frac{1}{(M+m)} \frac{M|\vec{k}|}{m\sqrt{q^2}} \{ (p+k) \cdot q (-A_0 + A_+) + q^2 A_- \} \\ H_\pm &= \epsilon^{\mu\dagger}(\pm) \epsilon_2^{\alpha\dagger}(\pm) \mathcal{H}_{\mu\alpha} \\ &= \frac{1}{(M+m)} \{ - (p+k) \cdot q A_0 \mp 2M|\vec{k}|V \} \\ H_0 &= \epsilon^{\mu\dagger}(0) \epsilon_2^{\alpha\dagger}(0) \mathcal{H}_{\mu\alpha} \\ &= \frac{1}{(M+m)} \frac{1}{2m\sqrt{q^2}} \{ - (p+k) \cdot q (M^2 - m^2 - q^2) A_0 + 4M^2 |\vec{k}|^2 A_+ \} \end{aligned} \quad (24)$$

3. Results & Analysis

To accurately describe the present processes under investigation we use the following input parameters as stated in Table 1. With this set of input parameters the Lorentz invariant form factors in (18) are obtained from the overlap integrals of meson wave functions. These form factors depend

Quarks	Mass (GeV)	Binding Energy (GeV)	Mass: Mesons & Leptons (MeV/GeV)
b	4.77659	4.76633	B^0 (5279.63), B^+ (5279.34), B_s (5366.9), B_c (6274.47), τ (1776.86)
c	1.49276	1.57951	D^0 (1864.84), D^{0*} (2006.85), D^- (1869.66), D^{*-} (2010.26), D_s (1968.34), D_s^* (2112.2)
u	0.07875	0.47125	η_c (2983.9), J/ψ (3096.9)
s	0.31575	0.59100	
Other inputs: $(a, V_0) = (0.017166 \text{ GeV}^3, -0.1375 \text{ GeV})$, $V_{cb} = 0.0408 \pm 0.0014$, $V_{ub} = 0.00382 \pm 0.00020$, $\tau_{B_c} = 0.51 \pm 0.009 \text{ ps}$, $\tau_{B_s} = 1.516 \pm 0.009 \text{ ps}$			

Table 1: Input parameters used in the analysis: quark masses, masses of mesons and τ lepton, CKM elements, and lifetimes.

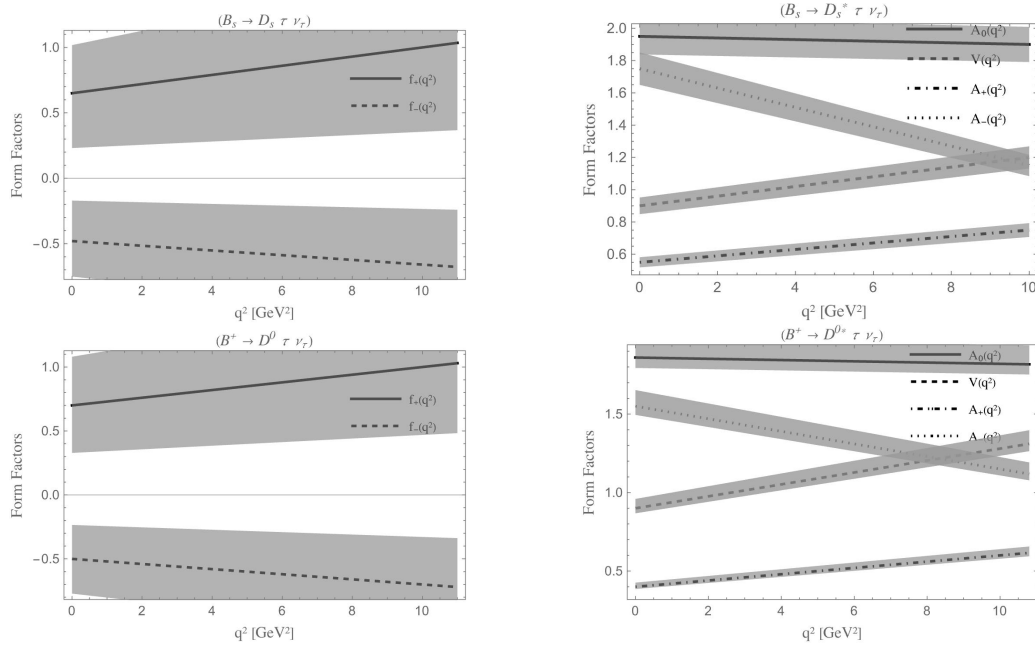


Figure 3: q^2 distribution spectra of the form factors for $B_s \rightarrow D_s^{(*)} \tau \nu_\tau$ and $B \rightarrow D^{(*)} \tau \nu_\tau$ transition

on the squared momentum transfer $q^2 = (p_B - p_X)^2$, varying within $q_{\min}^2 = 0$ to $q_{\max}^2 = (M_B - m_X)^2$. For $0^- \rightarrow 0^-$ transitions, the dominant contributions arise from $f_+(q^2)$ and $f_-(q^2)$ describing vector currents. For $0^- \rightarrow 1^-$ form factors $V(q^2)$, $A_0(q^2)$, $A_+(q^2)$, and $A_-(q^2)$ account for vector and axial-vector components due to spin-1 nature of the final meson. Fig. 3 shows the q^2 -dependence of the form factors for $B \rightarrow D^{(*)} \tau \nu_\tau$ and $B_s \rightarrow D_s^{(*)} \tau \nu_\tau$. The form factor $f_+(q^2)$ increases monotonically up to $\sim 11 \text{ GeV}^2$ while $f_-(q^2)$ decreases with q^2 consistent with HQET and pole-dominance expectations [20, 21]. The dominance of $f_+(q^2)$ is enhanced for τ modes due to reduced phase space at large q^2 . A similar pattern holds for $B_s \rightarrow D_s$, though with slightly larger $f_+(q^2)$ values reflecting internal quark dynamics. For $B \rightarrow D^*$ and $B_s \rightarrow D_s^*$ transitions, $A_0(q^2)$ remains

nearly constant, indicating weak q^2 dependence of the scalar axial current contribution which governs longitudinal polarization. The $V(q^2)$ and $A_+(q^2)$ form factors rise with recoil while $A_-(q^2)$ decreases due to kinematic suppression. Overall trends align with the covariant light-front quark model [22] and are consistent with PQCD [23] and LQCD predictions [24–27] with deviations within model uncertainties. Symmetry-breaking effects between $B \rightarrow D^{(*)}$ and $B_s \rightarrow D_s^{(*)}$ remain below 10% [23]. Compared with BCL [28, 29] or z -expansion parameterizations, our RIQ model agrees within 5–10% at low to moderate q^2 with larger deviations near q_{max}^2 due to parametrization sensitivity. A key advantage of our model is its ability to compute form factors over the full q^2 range without extrapolation serving inputs to helicity amplitudes for evaluating branching ratios and angular asymmetries outlined below in Table 2, 3 & 4. The total branching fractions are

Channels	This work	PQCD [23, 30]	PQCD+Lattice [23]	LQCD [31–35]	RQM [36]	RCQM [37]	LCSR [38]	HQET [39]	PDG [40]
$B^+ \rightarrow D^0 \tau^+ \nu_\tau$	$0.81^{+0.44}_{-0.43}$	$0.86^{+0.34}_{-0.25}$	$0.69^{+0.21}_{-0.17}$	0.65 ± 0.04	–	–	–	0.66 ± 0.05	0.77 ± 0.25
$B^+ \rightarrow D^{0*} \tau^+ \nu_\tau$	$1.96^{+0.13}_{-0.07}$	$1.60^{+0.39}_{-0.37}$	$1.34^{+0.26}_{-0.23}$	1.22 ± 0.07	–	–	–	1.43 ± 0.05	1.88 ± 0.20
$B^0 \rightarrow D^- \tau^+ \nu_\tau$	$0.75^{+0.40}_{-0.41}$	$0.82^{+0.33}_{-0.24}$	$0.62^{+0.19}_{-0.14}$	–	–	–	–	0.64 ± 0.05	0.99 ± 0.21
$B^0 \rightarrow D^{*-} \tau^+ \nu_\tau$	$1.81^{+0.12}_{-0.07}$	$1.53^{+0.37}_{-0.35}$	$1.25^{+0.25}_{-0.21}$	–	–	–	–	1.29 ± 0.06	1.45 ± 0.10
$B_s \rightarrow D_s \tau \nu_\tau$	$0.76^{+0.43}_{-0.49}$	$0.72^{+0.32}_{-0.23}$	$0.63^{+0.17}_{-0.13}$	0.74 ± 0.06	0.62 ± 0.05	–	$0.33^{+0.14}_{-0.11}$	–	–
$B_s \rightarrow D_s^* \tau \nu_\tau$	$1.83^{+0.11}_{-0.10}$	$1.45^{+0.46}_{-0.40}$	$1.20^{+0.26}_{-0.23}$	1.25 ± 0.05	1.3 ± 0.1	–	–	–	–
$B_c \rightarrow \eta_c \tau \nu_\tau$	$0.16^{+0.3}_{-0.2}$	$0.27^{+0.84}_{-0.63}$	$0.24^{+0.49}_{-0.40}$	–	–	0.22	$0.26^{+0.6}_{-0.5}$	–	–
$B_c \rightarrow J/\psi \tau \nu_\tau$	$0.56^{+0.5}_{-0.41}$	$0.45^{+1.29}_{-1.01}$	$0.38^{+0.63}_{-0.58}$	$0.41(3)$	–	0.49	$0.53^{+1.6}_{-1.4}$	–	–
$B_c \rightarrow D \tau \nu_\tau$	$0.0029^{+0.82}_{-0.69}$	$0.0022^{+0.72}_{-0.52}$	–	$0.0023(23)$	–	0.0021	–	–	–
$B_c \rightarrow D^* \tau \nu_\tau$	$0.023^{+0.13}_{-0.12}$	$0.0064^{+0.20}_{-0.16}$	–	–	–	0.0022	–	–	–

Table 2: RIQM predictions for the branching fractions (in units of 10^{-2}).

obtained by integrating the differential decay rate (22). Table 2 lists our predictions (in units of 10^{-2}) alongside results from PQCD [23], LQCD [31–33], LCSR [38], HQET [39], and quark models [36, 37]. Uncertainties include $\pm 5\%$ variation from model parameters (a , V_0) and PDG input errors. Our RIQ model predictions agree well with the available PDG data [40] and remain within theoretical and experimental bounds. For $B^+ \rightarrow D^0$ and $B_s \rightarrow D_s$ decays, no direct LQCD results exist for absolute branching fractions therefore we estimate them using lattice-predicted ratios \mathcal{R}_D and \mathcal{R}_{D_s} [32, 33] and experimental $\mathcal{B}(B \rightarrow D(D_s) \ell \nu_\ell)$, finding good consistency, especially for $B_s \rightarrow D_s$. Channels with $J^P = 1^-$ final states show slightly enhanced branching fractions compared to $J^P = 0^+$, reflecting relativistic and spin-structure effects. The close agreement across B and B_s decays implies mild SU(3) breaking ($< 10\%$) [41].

Using the central value of the B_c meson lifetime, we also determine the branching fractions for the semitauonic B_c decays into charmonium and charm meson final states. Overall the values obtained from Relativistic Constituent Quark Model [37] lie within the same order of magnitude. Consistent with the expectations from various theoretical approaches, we find $\mathcal{B}(B_c \rightarrow J/\psi)$ is in good agreement with the results reported in Refs. [35, 37]. For $B_c \rightarrow \eta_c$ channel our prediction is lower by a factor of ~ 2 compared with Refs. [37] but is consistent with the estimates in [37]. As anticipated, branching fractions for $B_c \rightarrow D^{(*)}$ modes arising from the underlying $b \rightarrow u$ transition are significantly smaller than those involving in charmonium final states. Our result for $B_c \rightarrow D$ decay are consistent with the predictions reported by LQCD [34]. For $B_c \rightarrow D^*$ transition our values are larger in comparison with Refs. [30, 37] by a factor of ~ 5 . Predictions for $B_c \rightarrow D^*$ and $B_c \rightarrow \eta_c$ serve as useful benchmarks in the absence of Lattice data supporting the

robustness of the RIQM across pseudoscalar and vector transitions. Using the computed form fac-

Observable	Approach	$B^0 \rightarrow D^- \tau^+ \nu_\tau$	$B_s^0 \rightarrow D_s^- \tau^+ \nu_\tau$	$B^0 \rightarrow D^{*-} \tau^+ \nu_\tau$	$B_s^0 \rightarrow D_s^{*-} \tau^+ \nu_\tau$
$P_\tau(D_{(s)}^*)$	This Work	0.293	0.291	-0.53	-0.53
	LQCD[31]	—	—	-0.54(19)	-0.53(91)
	PQCD [23]	0.32(1)	0.31(1)	-0.54(1)	-0.54(1)
	Belle[1]	—	$-0.38 \pm 0.51^{+0.21}_{-0.16}$	—	—
$F_L(D_{(s)}^*)$	This Work	—	—	0.48	0.48
	LQCD[31]	—	—	0.39(24)	0.42(12)
	PQCD [23]	—	—	0.42(1)	0.42(1)
	Belle[2]	—	—	$0.60 \pm 0.08 \pm 0.04$	—
	LHCb[5]	—	—	$0.41 \pm 0.06 \pm 0.03$	—

Table 3: RIQM predictions vs SM and data for $P_\tau(D_{(s)}^*)$ and $F_L(D_{(s)}^*)$

tors the angular observables: Forward-Backward asymmetry (\mathcal{A}_{FB}), asymmetry parameter (F_L) which determines the transverse and longitudinal composition of the vector meson final state and longitudinal τ polarization ($\langle P_L^\tau \rangle$) for the semitauonic B , B_s and B_c decays modes are also evaluated. Table 3 summarizes our results consistent with SM-based predictions and Belle data [1] despite large experimental uncertainties. These observables are far more sensitive to the underlying theoretical framework than the total decay rate. $F_L(D^*) = 0.48$ lies within 2σ of the Belle and LHCb averages [2, 5] indicating statistical agreement. Their precise measurement can therefore help distinguish between different theoretical models and provide valuable insight into the internal structure and nature of the B meson. These results further validate the reliability of our model in describing angular parameters.

Decay process	RIQ Model			Lattice QCD [42]		
	\mathcal{A}_{FB}	$\langle P_L^\tau \rangle$	F_L	\mathcal{A}_{FB}	$\langle P_L^\tau \rangle$	F_L
$B_c \rightarrow \eta_c \tau \nu$	0.357	0.28	—	—	—	—
$B_c \rightarrow J/\psi \tau \nu$	0.093	0.56	-0.066	-0.058(12)	0.5185(75)	0.4416(92)
$B_c \rightarrow D \tau \nu$	0.210	0.47	—	—	—	—
$B_c \rightarrow D^* \tau \nu$	0.137	0.14	-0.45	—	—	—

Table 4: Results of angular observables for B_c decays predicted by RIQM and available LQCD data.

Table 4 summarizes our model predictions of angular observables in the B_c decay channels. For transitions involving spin-1 final states, the transverse helicity contribution is significantly larger than the longitudinal one in the τ mode exceeding it by approximately a factor of two. In the case of the $B_c \rightarrow D^*$ transition the dominance of the transverse component becomes even more pronounced with an enhancement of nearly a factor of 7 in the τ^- mode. To quantify the relative strengths of the transverse and longitudinal polarizations of final vector mesons in the $B_c \rightarrow J/\psi$ and $B_c \rightarrow D^*$ decays, we evaluate the asymmetry observable F_L . For the $B_c \rightarrow J/\psi$ channel the resulting value is approximately -7% . In contrast for $B_c \rightarrow D^*$ transition our prediction yields a substantially larger negative value, reaching nearly -45% . This pronounced suppression arises from the fact

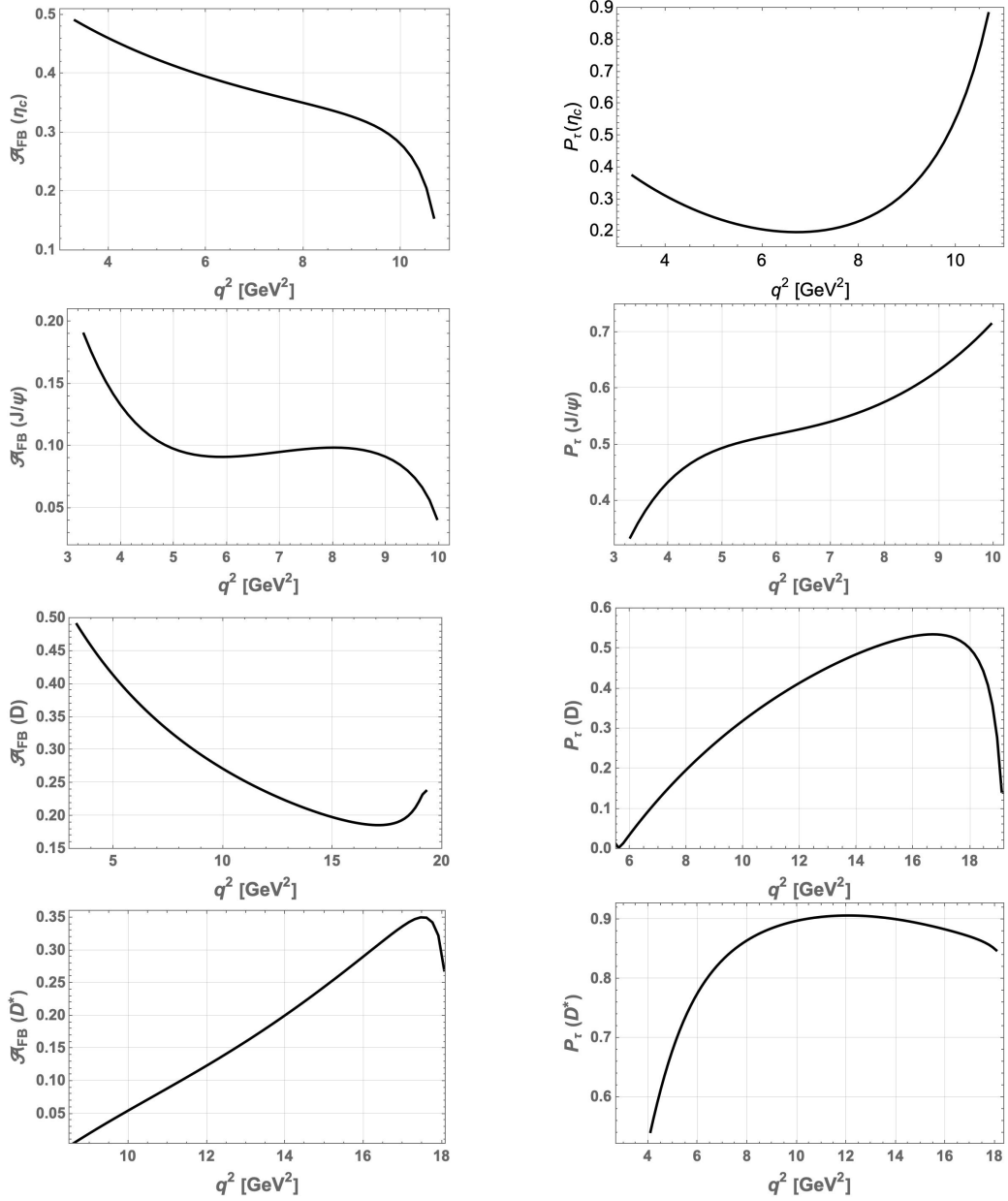


Figure 4: q^2 distribution spectra of the angular observables in B_c semitauponic decays

that, in the latter case the scalar-flip helicity amplitude \tilde{S} becomes the leading contribution and interferes destructively with the remaining amplitudes thereby driving the asymmetry parameter to such a strongly negative value. Our estimate for the τ -polarization $B_c \rightarrow J/\psi$ mode, $P_\tau(J/\psi)$, shows good agreement with the corresponding LQCD determinations reported in Refs. [35, 42]. Furthermore, the obtained value of $P_\tau(\eta_c) = -0.28$ exhibits qualitative compatibility with the results from the PQCD combined with lattice inputs presented in Ref. [43]. In addition, we present predictions of the observables in $B_c \rightarrow D$ and $B_c \rightarrow D^*$ for which LQCD results are currently not available. Hence our theoretical estimates may serve as a valuable reference for probing angular

observables in these charm final-states of B_c semitaauonic decays.

Fig. 4 depicts the q^2 distributions of forward-backward asymmetry and longitudinal τ -polarization in $B_c \rightarrow (J/\psi, \eta_c, D, D^*)$ decays. For the pseudoscalar transition $B_c \rightarrow \eta_c$ the τ -polarization spectra start near $q^2 \simeq 2 \text{ GeV}^2$ and decrease over $2 \leq q^2 \leq 8 \text{ GeV}^2$ due to limited phase space. Unlike $B_c \rightarrow D$ which grows smoothly with q^2 , the quantity $P_\tau(\eta_c)$ rises steadily at higher q^2 . This trend reflects the absence of the parity-odd helicity structure H_p in pseudoscalar amplitudes, leading to strong q^2 sensitivity across the spectrum. For $B_c \rightarrow (J/\psi, D^*)$, P_τ shows a rapid increase in the large q^2 region driven by the dominant no-flip part of the transverse helicity amplitude. The q^2 -dependence of $P_\tau(J/\psi)$ agrees qualitatively with Lattice predictions [42]. The q^2 distributions of \mathcal{A}_{FB} for η_c and D , the spectra falls near zero recoil while for J/ψ , it decreases at low q^2 upto $\sim 6 \text{ GeV}^2$ and then drops sharply at high q^2 due to the threshold factor $(q^2 - m_\tau^2)/q^2$ suppressing the longitudinal amplitude L . The shape of $\mathcal{A}_{\text{FB}}(J/\psi)$ is consistent with Lattice results [42]. For $B_c \rightarrow D^*$, the spin-flip contribution is small but the scalar flip term \tilde{S} becomes relevant at large q^2 shaping the overall behavior of $\mathcal{A}_{\text{FB}}(D^*)$.

4. Summary

The present investigation provide timely theoretical inputs & outcomes for ongoing and future experiments, offering insights into SM dynamics with continued synergy between phenomenology, Lattice studies and measurements being crucial for probing semileptonic heavy meson decays involving τ leptons. Further improvements can be made in this analysis by adopting a *correlated approach* where we will constrain the model parameters and extract the meson wavefunctions using LQCD inputs of $B_c \rightarrow J/\psi$ form factors. This Lattice-constrained framework will then be employed to compute the full q^2 dependence of form factors for a broader class of decay channels. By combining phenomenological modeling with robust non-perturbative inputs, this approach will significantly improve reliability over purely potential model based predictions.

References

- [1] **Belle** Collaboration, S. Hirose *et al.*, “Measurement of the τ lepton polarization and $R(D^*)$ in the decay $\bar{B} \rightarrow D^* \tau^- \bar{\nu}_\tau$,” *Phys. Rev. Lett.* **118** no. 21, (2017) 211801, [arXiv:1612.00529 \[hep-ex\]](#).
- [2] **Belle** Collaboration, A. Abdesselam *et al.*, “Measurement of the D^{*-} polarization in the decay $B^0 \rightarrow D^{*-} \tau^+ \nu_\tau$,” in *10th International Workshop on the CKM Unitarity Triangle*. 3, 2019. [arXiv:1903.03102 \[hep-ex\]](#).
- [3] Z.-R. Huang, Y. Li, C.-D. Lu, M. A. Paracha, and C. Wang, “Footprints of New Physics in $b \rightarrow c \tau \nu$ Transitions,” *Phys. Rev. D* **98** no. 9, (2018) 095018, [arXiv:1808.03565 \[hep-ph\]](#).
- [4] S. Bhattacharya, S. Nandi, and S. Kumar Patra, “ $b \rightarrow c \tau \nu_\tau$ Decays: a catalogue to compare, constrain, and correlate new physics effects,” *Eur. Phys. J. C* **79** no. 3, (2019) 268, [arXiv:1805.08222 \[hep-ph\]](#).

- [5] **LHCb** Collaboration, R. Aaij *et al.*, “Measurement of the D^* longitudinal polarization in $B^0 \rightarrow D^{*-} \tau^+ \nu_\tau$ decays,” [arXiv:2311.05224 \[hep-ex\]](#).
- [6] M. Y. Khlopov, “Effects of Symmetry Violation in Semileptonic Meson Decays,” *Sov. J. Nucl. Phys.* **28** (1978) 583.
- [7] C.-H. Chang and Y.-Q. Chen, “The Decays of $B(c)$ meson,” *Phys. Rev. D* **49** (1994) 3399–3411.
- [8] U. Dey and S. Nandi, “Correlated study on some $B_c \rightarrow P$ and $B_c \rightarrow S$ wave channels in light of new inputs,” *JHEP* **07** (2025) 144, [arXiv:2503.01693 \[hep-ph\]](#).
- [9] F. U. Bernlochner, M. F. Sevilla, D. J. Robinson, and G. Wormser, “Semitauonic b-hadron decays: A lepton flavor universality laboratory,” *Rev. Mod. Phys.* **94** no. 1, (2022) 015003, [arXiv:2101.08326 \[hep-ex\]](#).
- [10] L. Nayak, S. Patnaik, P. C. Dash, S. Kar, and N. Barik, “Lepton mass effects in exclusive semileptonic B_c -meson decays,” *Phys. Rev. D* **104** (2021) 036012, [arXiv:2106.09463 \[hep-ph\]](#).
- [11] L. Nayak, S. Patnaik, P. Sadangi, and S. K. Swain, “Study of exclusive decays of $B_s \rightarrow \psi(1S, 2S) K_s$ and $B_s \rightarrow \eta c(1S, 2S) K_s$,” *Phys. Rev. D* **110** no. 11, (2024) 113003, [arXiv:2404.14267 \[hep-ph\]](#).
- [12] S. Patnaik, P. C. Dash, S. Kar, S. Patra, and N. Barik, “Magnetic dipole transitions of B_c and B_c^* mesons in the relativistic independent quark model,” *Phys. Rev. D* **96** no. 11, (2017) 116010, [arXiv:1710.08242 \[hep-ph\]](#). [Erratum: *Phys.Rev.D* 99, 019901 (2019)].
- [13] S. Patnaik, L. Nayak, P. Sadangi, S. Swain, and R. Singh, “Study of angular observables in exclusive semileptonic B_c decays,” *Phys. Rev. D* **110** no. 5, (2024) 055028, [arXiv:2312.17114 \[hep-ph\]](#).
- [14] S. Patnaik, L. Nayak, and S. K. Swain, “ $B \rightarrow D^{(*)} \tau \nu \tau$ decay properties with the relativistic independent quark model,” *Phys. Rev. D* **112** no. 3, (2025) 033003.
- [15] N. Barik and B. K. Dash, “Mass Spectrum of Low Lying Baryons in the Ground State in a Relativistic Potential Model of Independent Quarks With Chiral Symmetry,” *Phys. Rev. D* **33** (1986) 1925–1933.
- [16] N. Barik, B. K. Dash, and P. C. Dash, “The $(Q\bar{Q})$ Pion and Its Decay Constant in a Chiral Potential Model,” *Pramana* **29** (1987) 543–557.
- [17] C. W. Wong, “Center-of-mass Correction in the MIT Bag Model. 2.” *Phys. Rev. D* **24** (1981) 1416.
- [18] L. Nayak, S. Patnaik, D. Pandey, and S. K. Swain, “Mass spectrum of S-wave mesons in the relativistic independent quark model,” [arXiv:2504.05714 \[hep-ph\]](#).

- [19] K. Dash, P. C. Dash, R. N. Panda, S. Kar, and N. Barik, “Purely leptonic decays of heavy-flavored charged mesons,” *Phys. Rev. D* **110** no. 5, (2024) 053004, arXiv:2312.06130 [hep-ph].
- [20] W. Wang, Y.-L. Shen, and C.-D. Lu, “Covariant Light-Front Approach for $B(c)$ transition form factors,” *Phys. Rev. D* **79** (2009) 054012, arXiv:0811.3748 [hep-ph].
- [21] Y.-Y. Fan, W.-F. Wang, and Z.-J. Xiao, “Study of $\bar{B}_s^0 \rightarrow (D_s^+, D_s^{*+})l^- \bar{\nu}_l$ decays in the pQCD factorization approach,” *Phys. Rev. D* **89** no. 1, (2014) 014030, arXiv:1311.4965 [hep-ph].
- [22] R. C. Verma, “Decay constants and form factors of s-wave and p-wave mesons in the covariant light-front quark model,” *J. Phys. G* **39** (2012) 025005, arXiv:1103.2973 [hep-ph].
- [23] X.-Q. Hu, S.-P. Jin, and Z.-J. Xiao, “Semileptonic decays $B/B_s \rightarrow (D^{(*)}, D_s^{(*)})l\nu_l$ in the PQCD approach with the lattice QCD input,” *Chin. Phys. C* **44** no. 5, (2020) 053102, arXiv:1912.03981 [hep-ph].
- [24] **HPQCD** Collaboration, J. Harrison, C. Davies, and M. Wingate, “Lattice QCD calculation of the $B_{(s)} \rightarrow D_{(s)}^* \ell \nu$ form factors at zero recoil and implications for $|V_{cb}|$,” *Phys. Rev. D* **97** no. 5, (2018) 054502, arXiv:1711.11013 [hep-lat].
- [25] B. Blossier, P. H. Cahue, J. Heitger, S. La Cesa, J. Neuendorf, and S. Zafeiropoulos, “ $B_s \rightarrow D_s^{(*)}$ form factors from lattice QCD with $N_f = 2$ Wilson-clover quarks,” *PoS LATTICE2021* (2022) 056, arXiv:2111.05733 [hep-lat].
- [26] **HPQCD** Collaboration, J. Harrison and C. T. H. Davies, “ $B_s \rightarrow D_s^*$ form factors for the full q^2 range from lattice QCD,” *Phys. Rev. D* **105** no. 9, (2022) 094506, arXiv:2105.11433 [hep-lat].
- [27] **JLQCD** Collaboration, Y. Aoki, B. Colquhoun, H. Fukaya, S. Hashimoto, T. Kaneko, R. Kellermann, J. Koponen, and E. Kou, “ $B \rightarrow D^* \ell \nu \ell$ semileptonic form factors from lattice QCD with Möbius domain-wall quarks,” *Phys. Rev. D* **109** no. 7, (2024) 074503, arXiv:2306.05657 [hep-lat].
- [28] Y.-Y. Fan, W.-F. Wang, S. Cheng, and Z.-J. Xiao, “Semileptonic decays $B \rightarrow D^{(*)}l\nu$ in the perturbative QCD factorization approach,” *Chin. Sci. Bull.* **59** (2014) 125–132, arXiv:1301.6246 [hep-ph].
- [29] C. G. Boyd, B. Grinstein, and R. F. Lebed, “Model independent determinations of anti- $B \rightarrow D$ (lepton), D^* (lepton) anti-neutrino form-factors,” *Nucl. Phys. B* **461** (1996) 493–511, arXiv:hep-ph/9508211.
- [30] W.-F. Wang, X. Yu, C.-D. Lü, and Z.-J. Xiao, “Semileptonic decays $B_c^+ \rightarrow D_{(s)}^{(*)}(l^+l^-, l^+l^-)$ in the perturbative QCD approach,” *Phys. Rev. D* **90** no. 9, (2014) 094018, arXiv:1401.0391 [hep-ph].
- [31] **HPQCD, (HPQCD Collaboration)†** Collaboration, J. Harrison and C. T. H. Davies, “ $B \rightarrow D^*$ and $B_s \rightarrow D_s^*$ vector, axial-vector and tensor form factors for the full q^2 range from lattice QCD,” *Phys. Rev. D* **109** no. 9, (2024) 094515, arXiv:2304.03137 [hep-lat].

- [32] **MILC** Collaboration, J. A. Bailey *et al.*, “ $B \rightarrow D\ell\nu$ form factors at nonzero recoil and $|V_{cb}|$ from 2+1-flavor lattice QCD,” *Phys. Rev. D* **92** no. 3, (2015) 034506, arXiv:1503.07237 [hep-lat].
- [33] E. McLean, C. T. H. Davies, J. Koponen, and A. T. Lytle, “ $B_s \rightarrow D_s\ell\nu$ Form Factors for the full q^2 range from Lattice QCD with non-perturbatively normalized currents,” *Phys. Rev. D* **101** no. 7, (2020) 074513, arXiv:1906.00701 [hep-lat].
- [34] **HPQCD** Collaboration, L. J. Cooper, C. T. H. Davies, and M. Wingate, “Form factors for the processes $B_c^+ \rightarrow D^0\ell^+\nu_\ell$ and $B_c^+ \rightarrow D_s^+\ell^+\ell^+(\nu\bar{\nu})$ from lattice QCD,” *Phys. Rev. D* **105** no. 1, (2022) 014503, arXiv:2108.11242 [hep-lat].
- [35] **HPQCD** Collaboration, J. Harrison, C. T. H. Davies, and A. Lytle, “ $B_c \rightarrow J/\psi$ form factors for the full q^2 range from lattice QCD,” *Phys. Rev. D* **102** no. 9, (2020) 094518, arXiv:2007.06957 [hep-lat].
- [36] R. N. Faustov and V. O. Galkin, “Weak decays of B_s mesons to D_s mesons in the relativistic quark model,” *Phys. Rev. D* **87** no. 3, (2013) 034033, arXiv:1212.3167 [hep-ph].
- [37] M. A. Ivanov, J. G. Korner, and P. Santorelli, “Exclusive semileptonic and nonleptonic decays of the B_c meson,” *Phys. Rev. D* **73** (2006) 054024, arXiv:hep-ph/0602050.
- [38] R.-H. Li, C.-D. Lu, and Y.-M. Wang, “Exclusive B_s decays to the charmed mesons $D_s^+(1968,2317)$ in the standard model,” *Phys. Rev. D* **80** (2009) 014005, arXiv:0905.3259 [hep-ph].
- [39] S. Fajfer, J. F. Kamenik, and I. Nisandzic, “On the $B \rightarrow D^*\tau\bar{\nu}_\tau$ Sensitivity to New Physics,” *Phys. Rev. D* **85** (2012) 094025, arXiv:1203.2654 [hep-ph].
- [40] **Particle Data Group** Collaboration, S. Navas *et al.*, “Review of particle physics,” *Phys. Rev. D* **110** no. 3, (2024) 030001.
- [41] M. Bordone, N. Gubernari, D. van Dyk, and M. Jung, “Heavy-Quark expansion for $\bar{B}_s \rightarrow D_s^{(*)}$ form factors and unitarity bounds beyond the $SU(3)_F$ limit,” *Eur. Phys. J. C* **80** no. 4, (2020) 347, arXiv:1912.09335 [hep-ph].
- [42] **LATTICE-HPQCD** Collaboration, J. Harrison, C. T. H. Davies, and A. Lytle, “ $R(J/\psi)$ and $B_c^- \rightarrow J/\psi\ell^-\bar{\nu}_\ell$ Lepton Flavor Universality Violating Observables from Lattice QCD,” *Phys. Rev. Lett.* **125** no. 22, (2020) 222003, arXiv:2007.06956 [hep-lat].
- [43] X.-Q. Hu, S.-P. Jin, and Z.-J. Xiao, “Semileptonic decays $B_c \rightarrow (\eta_c, J/\psi)l\bar{\nu}_l$ in the “PQCD + Lattice” approach,” *Chin. Phys. C* **44** no. 2, (2020) 023104, arXiv:1904.07530 [hep-ph].